Test Rig Landing Gear Free-Fall System Model Simulation and Design Optimization Using Matlab®

Mário Maia Neto and Luiz Carlos Sandoval Góes

Department of Mechanical Engineering, Aeronautical Institute of Technology, São José dos Campos, SP, Brazil
E-mail: mario.maia.neto@gmail.com, goes@ita.br

Abstract

In order to comply with the safety level demanded by civil certification requirements and military standards, alternative methods of extending retractable landing gear are provided in practically all airplanes of this type currently flying throughout the world. However, the emergency extension operation system design is not unique and architectures comprising simpler systems like free-fall or spring-assisted up to more complex systems like auxiliary hydraulics-assisted or pneumatics-assisted ones can be found in different airplanes. The airplane landing gear free-fall operation comprises a redundant, dissimilar and independent mechanically operated method of extending airplane landing gear due to a main hydraulic system failure or an electrical system malfunction. This paper aims at describing the modeling and simulation of a general landing gear emergency extension system built in a test rig, for a non-assisted type system, applying only an extension by gravity. Due to the low associated cost, satisfactory results and capability of easily assessing the trade-offs between different systems configurations, modeling applying computational software has become a frequent practice in aeronautical industries with the purpose of reducing product development cycle. Therefore, a parametric model of the landing gear emergency extension system was created in MATLAB® Simulink® and the system performance at nominal and particular operational conditions could be predicted by running several model simulations. Afterwards, through the assistance of MATLAB® tools, discrete and continuous optimization processes were accomplished to illustrate the benefits of applying these techniques to improve system operation response. An optimum damping condition permits the attenuation of the impact effects suffered by aircraft structure when landing gear falls by gravity in an emergency operation, as well as the assurance of sufficient energy for landing gear locking at the end of its downward movement.

Keywords: Landing Gear, Free-Fall, Modeling, Optimization

1 Introduction

Federal Aviation Regulations Part 23 and Part 25 and MIL-HDBK-516 are examples of civil and military standards frequently applied during the development and certification phases of these types of airplanes throughout the world. In order to guarantee an acceptable degree of safety level on landings, the aforementioned standards present requirements that states the aircraft shall comprise alternative methods of extending retractable landing gear in case of normal operation system failure. Their purpose consists in avoiding a wheels-up landing and it is potentially hazardous condition, as depicted in fig. 1.

According to [1], the landing gear design comprises more engineering disciplines than any other aircraft design topic. Knowledge about materials, manufacturing processes, electrical and hydraulic systems, mechanisms and even airfield strength is required to design the landing gear system.

Figure 1: A wheels-up landing. Source: [2]

The landing gear extension and retraction system choice is also a trade-off issue. For normal landing gear operation system, hydraulic systems consisting of accumulators, tubing, actuators and different types of valves, like restrictor, check and selector ones, represent the most used technology for this purpose. On the other hand, the emergency extension system design encompasses more types of architectures and therefore spring-assisted, auxiliary hydraulics-assisted, pneumatics-assisted or non-assisted free-fall design can be found in different airplanes of a same category.

The emergency free-fall system presents the simplest configuration, in which a lever or a knob installed in the cockpit is used by the pilot to unlock the landing gear and associated doors up locks, by means of cables, allowing the landing gear to fall by gravity. Basically, it consists in a redundant, dissimilar and independent mechanically operated method of extending airplane landing gear due to a main hydraulic system failure or an electrical system malfunction.

In aeronautical industries, the use of test rigs to accomplish systems operational tests has become a common practice before installing them in an aircraft prototype and running ground and flight tests. The systems integration test bench, usually known as ‘iron bird’, permits the execution of isolated and integrated systems tests, allowing the engineering team to predict deviations in a system operational performance when functioning lonely or simultaneously with other aircraft systems. Figure 2 illustrates an example of landing gear test rig.

Figure 2: A landing gear test rig. Source: [3]

On the other hand, performing system architecture changes during the rig test phase may lead to additional costs to the aircraft development program. Aiming to mitigate this risk, system modeling and optimization applying computational software have become a frequent practice in industries with the purpose of also reducing product development cycle. Due to the low associated cost, satisfactory results and capability of easily assessing the trade-offs between different systems configurations, the virtual modeling allows the predict of system performance at different operational conditions and facilitates the application of optimization techniques, hence reducing the possibility of a necessary system redesign in advanced stages of new aircraft development processes.

The free-fall system to be modeled is associated with a general landing gear emergency extension system built in a test rig. Due to the commonly restrictive operational envelope applicable to the landing gear emergency extension capability, merely a 1g flight test campaign is generally required by advisory circulars like [4] to show compliance with related certification regulations. Therefore, the current model could be further improved to take into consideration the aerodynamic and maneuver inertial effects occurring during flight in order to define and even expand the landing gear emergency operation envelope to be included in aircraft flight manual.

Finally, the provided model would be worth as a simple and quick evaluation tool to design the main components of the related hydraulic system and to define the variables to be measured during the system operational tests accomplished in production line applying hydraulic bench and aircraft lift on jacks.

Figure 3 presents the free-fall system schematics under evaluation. As depicted in the hydraulic diagram, the elements that make up the system are: nose landing gear, main landing gear (right and left), restrictor valves, tubing, selector valve, free-fall valve, uplocks and emergency lever. However, since the simulations are considered to initiate with the emergency lever pulled and all uplocks released, and the landing gear legs are assumed to be down locked after reaching a predetermined extension angle, the uplock and downlock mechanisms will not be modeled.

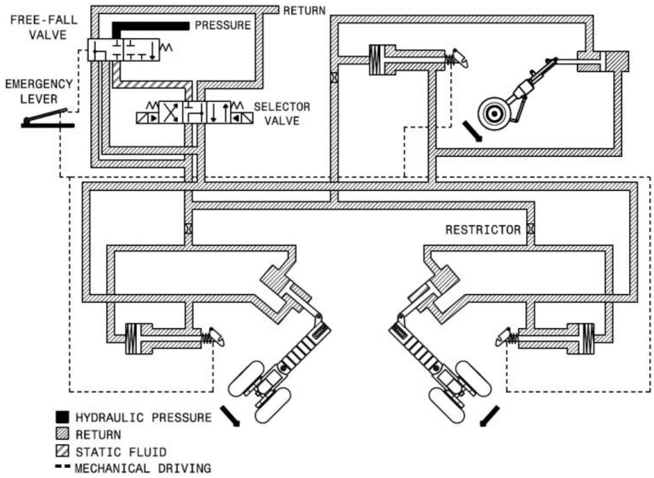

Figure 3: Landing gear free-fall system. Source: adapted from [5]

2 Formulation

The basic formulation that composes the free-fall system model will be divided into two separated topics: the hydraulic system equations and the landing gear dynamics ones.

2.1 Hydraulic System Modeling

A lumped element model is applied to the landing gear associated hydraulic system, which is characterized by the segregation of system important behavior effects like compliance, inertance and pressure drop, as well as the isolated components installed in the system such as valves and actuators, as discrete elements connected by means of the continuity law or specific pressure conditions. Nowadays, this methodology is embedded in modeling computational pieces of software like MATLAB® Simulink® Simscape library and allows the user a good comprehension of the relation between system components and their main effects.

Assuming at first no significant temperature variations in the system, constant values for fluid viscosity and density are used. However, the fluid density also exhibits a pressure-dependence variation, whose effect can be represented by a discrete element called “system compliance”. The ideal compliance is related to fluid flow and line pressure through eq. (1) [6]. Besides the fluid compressibility, the effects of entrapped air in hydraulic line and the tubing flexibility can also be considered in the calculation of the “effective bulk modulus” by means of eq. (2) [3][7].

$$C_f = \frac{A\,L}{\beta_e} \triangleq \frac{\int Q dt}{P} \tag{1}$$

$$\frac{1}{\beta_e} = \frac{1}{\beta_C} + \frac{1}{\beta_L} + \frac{V_G}{V_T}\left(\frac{1}{\beta_G} - \frac{1}{\beta_L}\right) \tag{2}$$

Due to its kinetic energy, the fluid flow exhibits another effect known as “fluid inertance”. Represented as another lumped element, the relation between pressure variation and fluid flow in the fluid inertance element is given by eq. (3) [6].

$$\Delta P \triangleq I_f \frac{dQ}{dt} \tag{3}$$

A typical value used for the inertance parameter is present in eq. (4). This formulation is more applicable for turbulent flow regime, when the Reynolds number, calculated by eq. (5), is greater than 4000 [6][7].

$$I_f = \frac{\rho L}{A} \tag{4}$$

$$Re = \frac{\rho V D}{\mu} \tag{5}$$

The last effect observed in the flow dynamics through hydraulic pipes consists in the fluid resistance, also referred to as “pressure drop”. Again, the fluid pressure drop can be modeled as a discrete element, whose semi-empirical equation for horizontal straight tubing and completely developed flow is described by eq. (6). The first term in the right-hand side of the equation is called the “friction factor” and is dependent on tubing relative roughness and also on Reynolds number [7].

$$\Delta P = f \frac{L}{D}\frac{\rho V^2}{2} \tag{6}$$

Components like restrictor and selector valves result in locally situated pressure drops. The relation between the fluid flow and the pressure drop through their orifices can be expressed by a non-linear equation for turbulent flows, as shown in eq. (7), or by a linear equation for laminar flows, given by eq. (8) [7].

$$Q = C_d A_o \sqrt{\frac{2}{\rho}(\Delta P)} \tag{7}$$

$$Q = \frac{2\delta^2 D_0 A_o}{\mu}\,\Delta P \tag{8}$$

The hydraulic actuators shown in fig. 3, responsible for performing the connection between the hydraulic system and the landing gear mechanism, are of double-acting, single-rod type. The continuity equations applied to the actuator chambers yield to the formulation presented in eq. (9) and eq. (10). As it can be seen, internal and external leakages are being taken into account as linearly dependents to the pressure differences between the chambers and between each chamber and the external environment, respectively [7].

$$Q_1 - C_{ip}(P_1 - P_2) - C_{ep}P_1 = \frac{dV_1}{dt} + \frac{V_1}{\beta_e}\frac{dP_1}{dt} \tag{9}$$

$$C_{ip}(P_1 - P_2) - C_{ep}P_2 - Q_2 = \frac{dV_2}{dt} + \frac{V_2}{\beta_e}\frac{dP_2}{dt} \tag{10}$$

2.2 Landing Gear Dynamics Modeling

The own landing gear weight comprises the main responsible for the extension torque in a free-fall system. For a ground test, the weight torque is basically a function of the landing gear mass, the distance between its center of gravity and the landing gear-to-aircraft attachment (landing gear rotation axle), and the landing gear extension angle. Therefore, substituting the landing gear mechanism mass for an equivalent mass located in the center of gravity of the landing gear leg, the weight torque for each landing gear becomes defined as in eq. (11).

$$T = m\;g\;a\;cos(\alpha) \tag{11}$$

On the other hand, during this type of operation, some resistant forces act against landing gear downward rotation, decreasing the gravitational potential energy used by the landing gear to extend.

The first resistant torque is consequence of the friction existing in the landing mechanism bearings. In order to simplify the model, this effect is summarized in a term called “viscous friction torque”. Proportional to the extension velocity by a constant factor known as damping coefficient, the viscous friction torque can be expressed by eq. (12).

$$F = B.\dot{\alpha} \tag{12}$$

During the landing gear free-fall extension, another resistant torque appears in the system as a result of the internal flow created in the hydraulic system due to actuator piston movement. Assuming the piston mass and its friction as negligible, the actuator force is caused by the pressure difference existing between its chambers applied to the area of each side of the piston. Equation (13) denotes the actuator force.

$$h = P_1 A_{p1} - P_2 A_{p2} \tag{13}$$

Therefore, the hydraulic actuator torque is defined as in eq. (14). Since the torque arms and piston displacements are functions of the landing gear extension angles, the nose landing gear and main landing gear CAD drawings were used to determine the relationship between them by doing simulated measurements at some extension angle values. Applying the obtained data, parametric curves were then defined making use of cubic polynomial regression techniques.

$$H = \pm h \,.\, r \quad (14)$$

Finally, combining in Newton's second law the sum of the torques that act on each landing gear leg during free-fall extension, eq. (15) is obtained.

$$I\,\ddot{\alpha} = T - F + H \quad (15)$$

2.3 Block Diagram

Figure 4 presents the block diagram of the free-fall system shown in fig. 3. Due to system symmetry, the same parameters values were considered for main landing gear 1 and 2, that is, left-side and right-side.

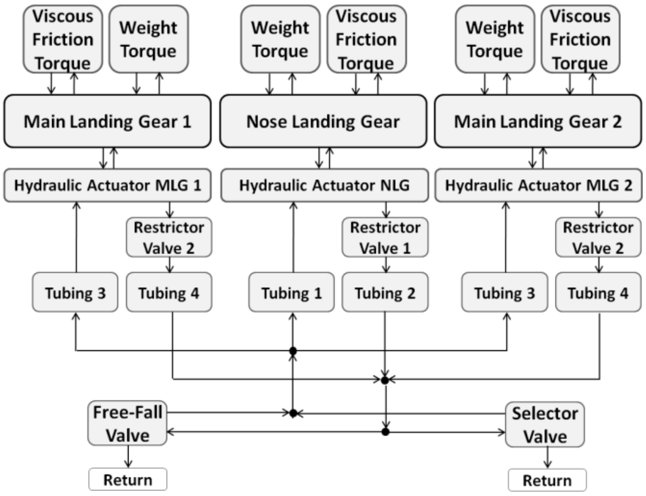

Figure 4: System block diagram. Source: adapted from [8] and [9]

Meanwhile the hydraulic system blocks are depicted in the bottom portion of the diagram, the applicable external torques are represented in the upper part, being the landing gear blocks the connection between them by means of Newton's second law. Regarding the system return pressure, which was assumed equal to the hydraulic fluid reservoir pressure, it basically represents the unique model boundary condition.

For all landing gear legs, it was adopted an extension angle range from 0° to 90° (π/2 radians). Since the downlock mechanism was not modeled, it was assumed as a particular criterion that, at an extension angle of 89° (1.533 radians), the landing gear is instantaneously locked supposedly by means of a mechanical lock, which brings it immediately to the final extension angle of 90° (π/2 radians).

Figure 5 illustrates the MATLAB® Simulink® model of the system. For the representation of tubing, restrictor valves, actuators and selector valve, as well as hydraulic fluid properties, the respective blocks from SimHydraulics® software were applied. Based on the Physical Network approach, SimHydraulics® comprises a modeling environment within Simulink® that is appropriate for hydraulic system design and control [10].

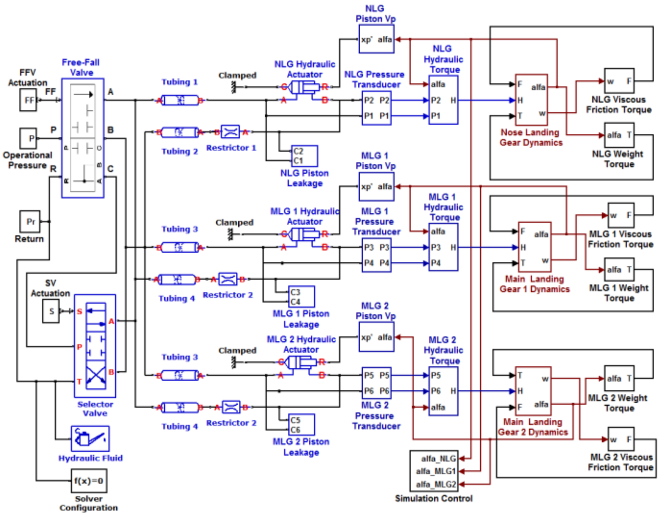

Figure 5: MATLAB® Simulink® model

A more detailed view of the hydraulic portion of landing gear operation system is shown in fig. 6. Taken from the SimHydraulics® pipeline library, the segmented pipeline block comprises all hydraulic important behavior effects like fluid compliance, inertance and resistance in a unique block. Concerning the internal and external leakages of the hydraulic actuators, their representation was accomplished by means of fixed orifice blocks located inside subsystem blocks referred to as "piston leakages", whose parameters were adjusted to maintain a laminar flow that kept the linear proportionality described in eq. (9) and eq. (10).

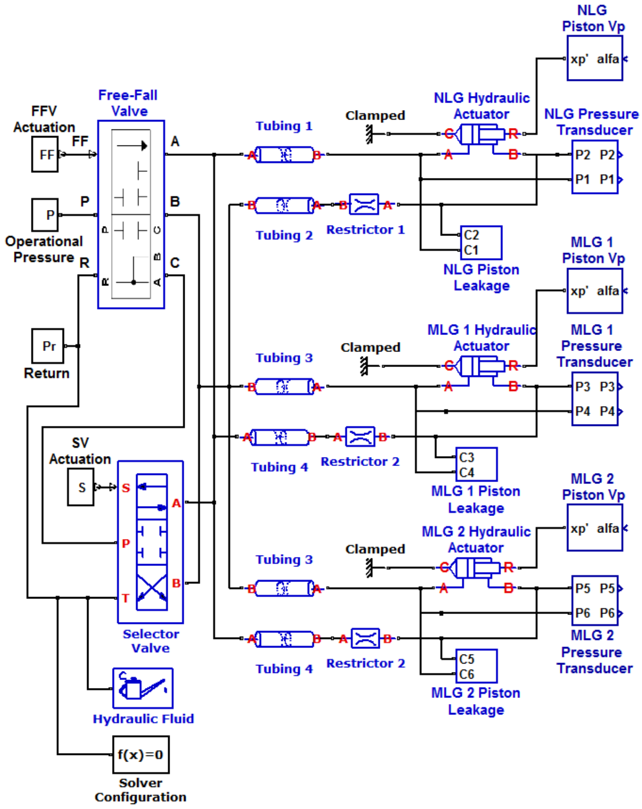

Figure 6 – Detailed view of landing gear system hydraulic components

3 Simulation Results

The simulation of the MATLAB® Simulink® model shown in fig. 5 was run applying the system parameters nominal values. To integrate the model differential equations, the simulation was configured to use a fixed-step solver known as “ode14x”. This implicit algorithm is a combination of Newton’s method and extrapolations from the current values [11]. The simulation step size was then adjusted in order to avoid convergence problems.

Figure 7 through fig. 10 present the development of the landing gear extension angles e respective velocities for nose and main landing gear. As illustrated especially by the velocities graphs, all landing gear legs demonstrated a similar extension profile for the ground test condition. However, the higher rotational velocity values during the first seconds of landing gear extension are consequence of the weight torque magnitude originated when the landing gear legs are practically in a horizontal position.

According to simulation results, the nose landing gear described a faster movement, taking 6.7 seconds to extend by free-fall. On the other hand, the main landing gear extension occurred in a slower manner, requiring 8.7 seconds to reach its final position.

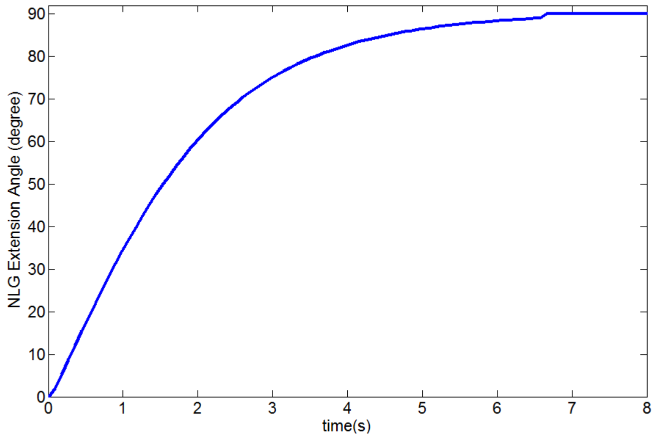

Figure 7: Nose landing gear extension angle: nominal simulation

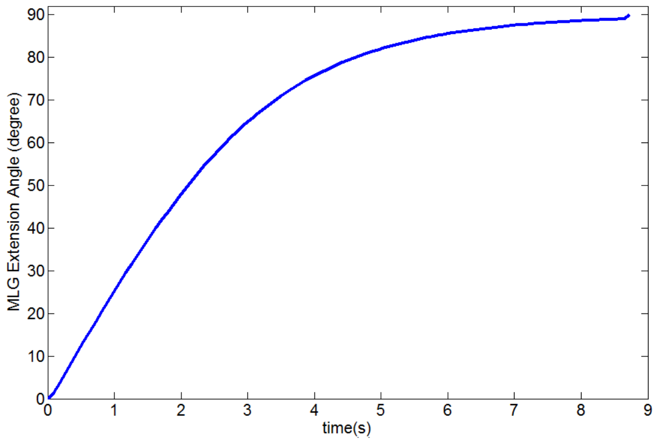

Figure 8: Main landing gear extension angle: nominal simulation

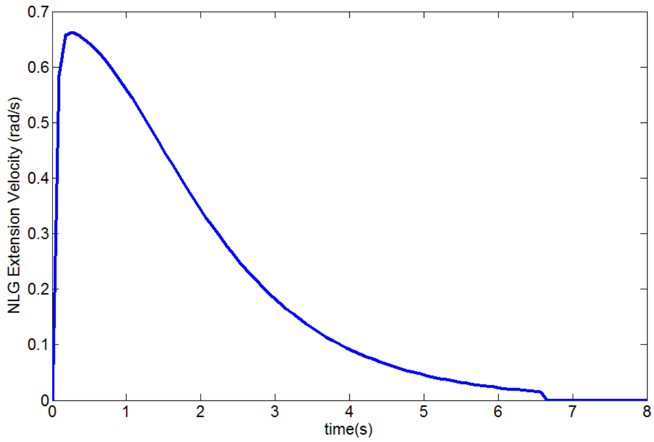

Figure 9: Nose landing gear extension velocity: nominal simulation

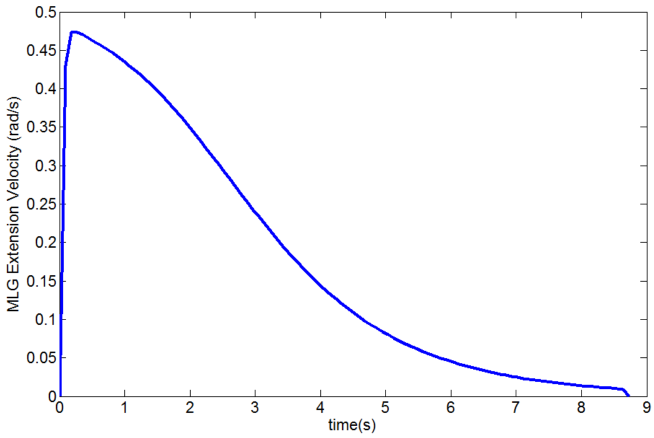

Figure 10: Main landing gear extension velocity: nominal simulation

The fluid temperature effect on landing gear extension times can be evaluated by means of fluid properties variation throughout hydraulic fluid temperature envelope. Assuming a fluid temperature range from -40ºC (-40ºF) to 66ºF (150ºF), the increase of landing gear emergency extension times at significant low fluid temperatures may be noticed in fig. 11, especially for main landing gear actuation.

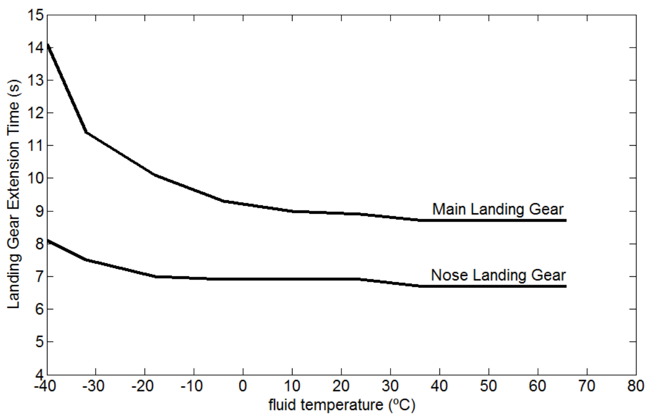

Figure 11: Fluid temperature effect on landing gear extension times

The impact of hydraulic fluid entrapped air on landing gear emergency extension performance can also be estimated using model simulation. For the present system, the consequence of a trapped air relative amount equal to 0.1 on main landing gear emergency extension is shown in fig. 12. Besides increasing extension time in approximately 0.5 second, the presence of a considerable quantity of trapped air in hydraulic fluid led to more oscillations in main landing gear velocities up to about 2 seconds as a result of the fluid capacitance rise. Finally, the existence of entrapped air in hydraulic system can affect not only the emergency extension system, but also landing gear normal retraction and extension operation, especially for those systems whose uplock and downlock mechanisms are very dependent on components synchronism.

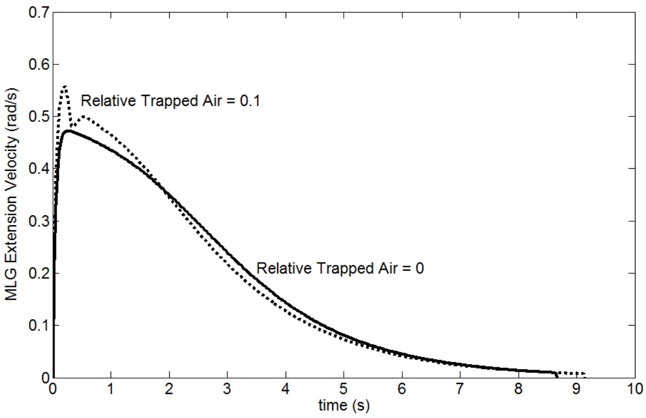

Figure 12 – Main landing gear extension velocities for two trapped air configurations

4 Model Optimization

Generally associated with competitive issues, quality assurance and manufacturing costs reduction, the aerospace design was among the earliest disciplines to significantly apply optimization processes in their product design due to the critical necessity of reducing weight in this type of vehicle. Nowadays, the success of applying an optimization process in engineering design demands not only a good mathematical model describing quantitatively the design problem, but also some specific knowledge from the designer like computer programming and optimization techniques [12].

The nominal simulation results shown in fig. 7 to fig. 10 present in such a way an example of what can be found in terms of free-fall operation. Not even the time delay between the final extensions of the landing gear legs, but also the impacts their movements may have on aircraft structure and landing safety are among the main concerns landing gear engineers have during the system design. While one landing gear leg may reach the lowest point with a considerable amount of energy, which eventually can cause structural damage to its attachment point, other landing gear leg may hardly get down and locked due to the small energy it has at the end of its movement, putting at risk the aircraft integrity in the subsequent landing.

The purpose of the following steps is to illustrate a practical optimization process in order to reduce the time delay between the extension of nose and main landing gear and, consequently, better adjusting the behavior they present at the end of their movements. For this purpose, it is assumed a rig test requirement for free-fall extension time of 7.0 seconds minimum and 8.2 seconds maximum at nominal environmental temperature.

The first example of system optimization considers a discrete optimization method. Although several continuous optimization algorithms are available nowadays in software like MATLAB®, the discrete optimization is also fundamental for engineering design problems, since in many situations the parameter value choice is associated with the standard dimensions provided by the suppliers in their catalogs or for some reason restricted due to manufacturing issues [12].

The “exhaustive enumeration” method comprises a discrete optimization technique, in which all solutions in search space are evaluated [12]. Its main drawback regarding the exponential increase in calculations as more variables are considered may not be a limitation at the present time due to the high memory and fast data processing capabilities of current computers. Moreover, this methodology allows the designer to observe the system response sensibility on parameter value variations throughout the optimization process.

Therefore, tab. 1 presents the parameters evaluated during the system discrete optimization process, as well as their nominal, minimum and maximum values considered in the algorithm. After running the iterative optimization, the parameter optimum values were obtained and are described in the last column of tab. 1.

Table 1: System parameters discrete optimization

Parameter	Nominal Value	Minimum Value	Maximum Value	Optimum Value
Restrictor 1 *(A_0)*	$2.54x10^{-6}$	$1.96x10^{-7}$	$7.07x10^{-6}$	$1.96x10^{-7}$
Restrictor 2 *(A_0)*	$2.54x10^{-6}$	$1.96x10^{-7}$	$7.07x10^{-6}$	$7.07x10^{-6}$
Tubing 1 *(D)*	$8.00x10^{-3}$	$4.00x10^{-3}$	$1.50x10^{-2}$	$4.00x10^{-3}$
Tubing 2 *(D)*	$8.00x10^{-3}$	$4.00x10^{-3}$	$1.50x10^{-2}$	$8.00x10^{-3}$
Tubing 3 *(D)*	$8.00x10^{-3}$	$4.00x10^{-3}$	$1.50x10^{-2}$	$1.50x10^{-2}$
Tubing 4 *(D)*	$8.00x10^{-3}$	$4.00x10^{-3}$	$1.50x10^{-2}$	$8.00x10^{-3}$
NLG Actuator *(A_{p1})*	$1.50x10^{-3}$	$1.30x10^{-3}$	$2.00x10^{-3}$	$1.30x10^{-3}$
NLG Actuator *(A_{p2})*	$1.00x10^{-3}$	$8.50x10^{-4}$	$1.25x10^{-3}$	$1.25x10^{-3}$
MLG Actuator *(A_{p1})*	$3.20x10^{-3}$	$2.60x10^{-3}$	$3.80x10^{-3}$	$2.60x10^{-3}$
MLG Actuator *(A_{p2})*	$1.70x10^{-3}$	$1.40x10^{-3}$	$2.51x10^{-3}$	$2.51x10^{-3}$

Table 2 illustrates the discrete optimization process applied in the present example. In order to reduce the simulation time, the landing gear emergency extension times were evaluated for each parameter configuration, starting from the nominal values denoted by a gray background in tab. 2, and switching the value of only a unique parameter to its maximum and minimum values at a time, in a cascade, successive matter. The optimum solution was found in line 18 of tab. 2.

On the other hand, aiming to assure the obtained result comprised the global optimum solution for the applicable search space, every allowable parameter value combination should have been analyzed, which would have led to more than 59,000 simulations. However, since the landing gear locking times after the proposed discrete optimization became 7.09 seconds for nose landing gear and 8.19 seconds for main landing, it was possible to meet the established requirements only making use of the 21 simulations shown in tab. 2.

Table 2: Discrete optimization process

Case	*Restrictor 1*	*Restrictor 2*	*Tubing 1*	*Tubing 2*	*Tubing 3*	*Tubing 4*	*NLG Actuator*	*NLG Actuator*	*MLG Actuator*	*MLG Actuator*	*NLG time (s)*	*MLG time (s)*
	A_0	A_0	D	D	D	D	A_{p1}	A_{p2}	A_{p1}	A_{p2}		
1	2.54×10^{-6}	2.54×10^{-6}	8.00×10^{-3}	8.00×10^{-3}	8.00×10^{-3}	8.00×10^{-3}	1.50×10^{-3}	1.00×10^{-3}	3.20×10^{-3}	1.70×10^{-3}	6.73	8.73
2	1.96×10^{-7}	2.54×10^{-6}	8.00×10^{-3}	8.00×10^{-3}	8.00×10^{-3}	8.00×10^{-3}	1.50×10^{-3}	1.00×10^{-3}	3.20×10^{-3}	1.70×10^{-3}	6.82	8.73
3	7.07×10^{-6}	2.54×10^{-6}	8.00×10^{-3}	8.00×10^{-3}	8.00×10^{-3}	8.00×10^{-3}	1.50×10^{-3}	1.00×10^{-3}	3.20×10^{-3}	1.70×10^{-3}	6.73	8.73
4	1.96×10^{-7}	1.96×10^{-7}	8.00×10^{-3}	8.00×10^{-3}	8.00×10^{-3}	8.00×10^{-3}	1.50×10^{-3}	1.00×10^{-3}	3.20×10^{-3}	1.70×10^{-3}	6.82	9.63
5	1.96×10^{-7}	7.07×10^{-6}	8.00×10^{-3}	8.00×10^{-3}	8.00×10^{-3}	8.00×10^{-3}	1.50×10^{-3}	1.00×10^{-3}	3.20×10^{-3}	1.70×10^{-3}	6.82	8.55
6	1.96×10^{-7}	7.07×10^{-6}	4.00×10^{-3}	8.00×10^{-3}	8.00×10^{-3}	8.00×10^{-3}	1.50×10^{-3}	1.00×10^{-3}	3.20×10^{-3}	1.70×10^{-3}	6.64	8.46
7	1.96×10^{-7}	7.07×10^{-6}	1.50×10^{-2}	8.00×10^{-3}	8.00×10^{-3}	8.00×10^{-3}	1.50×10^{-3}	1.00×10^{-3}	3.20×10^{-3}	1.70×10^{-3}	6.73	8.55
8	1.96×10^{-7}	7.07×10^{-6}	4.00×10^{-3}	4.00×10^{-3}	8.00×10^{-3}	8.00×10^{-3}	1.50×10^{-3}	1.00×10^{-3}	3.20×10^{-3}	1.70×10^{-3}	6.73	8.55
9	1.96×10^{-7}	7.07×10^{-6}	4.00×10^{-3}	1.50×10^{-2}	8.00×10^{-3}	8.00×10^{-3}	1.50×10^{-3}	1.00×10^{-3}	3.20×10^{-3}	1.70×10^{-3}	6.73	8.55
10	1.96×10^{-7}	7.07×10^{-6}	4.00×10^{-3}	8.00×10^{-3}	4.00×10^{-3}	8.00×10^{-3}	1.50×10^{-3}	1.00×10^{-3}	3.20×10^{-3}	1.70×10^{-3}	6.73	9.72
11	1.96×10^{-7}	7.07×10^{-6}	4.00×10^{-3}	8.00×10^{-3}	1.50×10^{-2}	8.00×10^{-3}	1.50×10^{-3}	1.00×10^{-3}	3.20×10^{-3}	1.70×10^{-3}	6.73	8.37
12	1.96×10^{-7}	7.07×10^{-6}	4.00×10^{-3}	8.00×10^{-3}	1.50×10^{-2}	4.00×10^{-3}	1.50×10^{-3}	1.00×10^{-3}	3.20×10^{-3}	1.70×10^{-3}	6.71	8.82
13	1.96×10^{-7}	7.07×10^{-6}	4.00×10^{-3}	8.00×10^{-3}	1.50×10^{-2}	1.50×10^{-2}	1.50×10^{-3}	1.00×10^{-3}	3.20×10^{-3}	1.70×10^{-3}	6.73	8.37
14	1.96×10^{-7}	7.07×10^{-6}	4.00×10^{-3}	8.00×10^{-3}	1.50×10^{-2}	8.00×10^{-3}	1.30×10^{-3}	1.00×10^{-3}	3.20×10^{-3}	1.70×10^{-3}	6.91	8.37
15	1.96×10^{-7}	7.07×10^{-6}	4.00×10^{-3}	8.00×10^{-3}	1.50×10^{-2}	8.00×10^{-3}	2.00×10^{-3}	1.00×10^{-3}	3.20×10^{-3}	1.70×10^{-3}	6.55	8.37
16	1.96×10^{-7}	7.07×10^{-6}	4.00×10^{-3}	8.00×10^{-3}	1.50×10^{-2}	8.00×10^{-3}	1.30×10^{-3}	8.50×10^{-4}	3.20×10^{-3}	1.70×10^{-3}	6.73	8.37
17	1.96×10^{-7}	7.07×10^{-6}	4.00×10^{-3}	8.00×10^{-3}	1.50×10^{-2}	8.00×10^{-3}	1.30×10^{-3}	1.25×10^{-3}	3.20×10^{-3}	1.70×10^{-3}	7.09	8.37
18	1.96×10^{-7}	7.07×10^{-6}	4.00×10^{-3}	8.00×10^{-3}	1.50×10^{-2}	8.00×10^{-3}	1.30×10^{-3}	1.25×10^{-3}	2.60×10^{-3}	1.70×10^{-3}	7.09	8.19
19	1.96×10^{-7}	7.07×10^{-6}	4.00×10^{-3}	8.00×10^{-3}	1.50×10^{-2}	8.00×10^{-3}	1.30×10^{-3}	1.25×10^{-3}	3.80×10^{-3}	1.70×10^{-3}	7.09	8.55
20	1.96×10^{-7}	7.07×10^{-6}	4.00×10^{-3}	8.00×10^{-3}	1.50×10^{-2}	8.00×10^{-3}	1.30×10^{-3}	1.25×10^{-3}	2.60×10^{-3}	1.40×10^{-3}	7.09	8.28
21	1.96×10^{-7}	7.07×10^{-6}	4.00×10^{-3}	8.00×10^{-3}	1.50×10^{-2}	8.00×10^{-3}	1.30×10^{-3}	1.25×10^{-3}	2.60×10^{-3}	2.51×10^{-3}	7.09	8.19

Another example of an optimization process in order to improve landing gear emergency extension performance, yet comprising continuous optimization, is demonstrated as follows.

As shown in fig. 11, the overall time for main landing gear to lock down at low hydraulic fluid temperatures can increase considerably if compared to a nominal operational temperature of about 37ºC (100ºF). Therefore, a continuous optimization technique is applied aiming to reduce the main landing gear extension time in at least 1.5 seconds at a hydraulic fluid operating temperature of -32ºC (-25ºF). According to fig. 11, the main landing gear took about 11.4 seconds to completely extend at the corresponding temperature.

For a MATLAB® Simulink® model, the use of a "Signal Constraint Block", taken from the Simulink Response Optimization library, facilitates significantly the user's workload when accomplishing a continuous optimization process. In order to optimize a variable response, the aforementioned block shall be linked to the respective signal of the Simulink® model and, by means of a graphical interface representation, have the signal amplitude limits defined by the user. As a result, by running the optimization algorithm, the selected design parameters values are adjusted to make the output signal obey the imposed bounds. Moreover, it is also possible to require that the variable response track a reference signal defined in the "Signal Constraint Block" user's interface [11].

Figure 13 presents the "Signal Constraint Block" applied to optimize the main landing gear emergency extension performance of the present model. The combination of the external torques in the left-side of fig. 13 are divided by the landing gear moment of inertia and then integrated twice to lead to the main landing gear extension angle. By means of a "Signal Constraint Block" linked to the main landing gear extension velocity signal, the respective variable response over the time can be enhanced through the application of the optimization process.

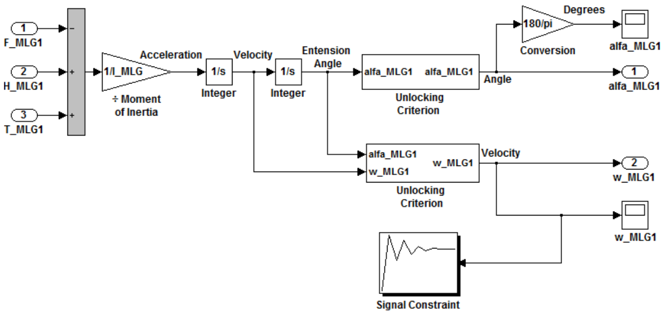

Figure 13 – Use of the "Signal Constraint Block" in main landing gear emergency extension optimization

For the present simulation, the "Signal Constraint Block" default optimization algorithm method called "gradient descent", applying a "medium scale" model size, was selected. The gradient descent algorithm makes use of MATLAB® Optimization Toolbox "fmincon" function to find the minimum of a nonlinear multivariable scalar function, subjected to predefined constraints in response signal and in design variable values, starting at an initial estimate. The "fmincon" function consists in a gradient-based method that applies finite difference techniques for calculation of function gradients. Concerning the option for a medium-scale model, it represents the solution of a quadratic programming subprogram and the use of a quasi-Newton approximation to calculate the Hessian of the Lagrangian at each iteration. Finally, the algorithm also allows the possibility of looking for the maximally feasible solution, which represents the finding of an optimal solution that is generally located further inside the constraint region instead of just closely satisfying the constraints [11].

The continuous system optimization was accomplished applying as design parameters three of the five component features associated with main landing gear actuation shown in tab. 1. Therefore, the orifice area of the restrictor valve located in main landing gear extension line and the tube diameters of both legs operation lines had their dimensions optimized in order to improve main landing gear emergency performance at low hydraulic fluid temperature. These parameters were selected due to the apparent convenience in updating their respective components, that is, restrictor valve and tubes, without more significant impacts.

As a result, the parameters evaluated during the system continuous optimization process, as well as their nominal and limit values, are present in tab. 3. The parameter optimum values obtained through the application of the "Signal Constraint Block" optimization algorithm are informed in the last column of tab. 3.

In order to obtain the optimum solution, the algorithm performed 4 iterations, accomplishing 28 objective function evaluations. The iteration results and the response signal imposed bounds applied during the optimization process are displayed in fig. 14. The white background area represents the allowable region for the output signal to stay within during the extension time interval.

Table 3: System design parameters applied in continuous optimization

Parameter	Nominal Value	Minimum Value	Maximum Value	Optimum Value
Restrictor 2 (A_0)	2.54×10^{-6}	1.96×10^{-7}	7.07×10^{-6}	7.07×10^{-6}
Tubing 3 (D)	8.00×10^{-3}	4.00×10^{-3}	1.50×10^{-2}	9.40×10^{-3}
Tubing 4 (D)	8.00×10^{-3}	4.00×10^{-3}	1.50×10^{-2}	1.38×10^{-2}

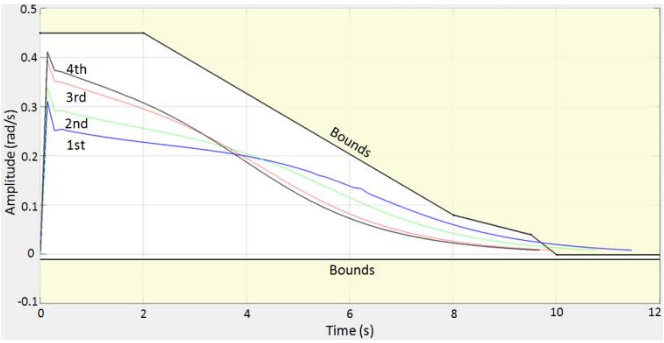

Figure 14 – "Signal Constraint Block" optimization result

Finally, considering the enhanced values obtained by means of the current optimization process for low hydraulic fluid temperature, the new landing gear free-fall extension times were 7.4 seconds and 9.7 seconds, for nose landing gear and main landing gear, respectively. Meanwhile for nose leg practically no improvement in extension time was achieved, which was expected since the design parameters chosen do not have direct effects on its performance, for main landing gear a reduction of 1.7 seconds in extension time was successfully obtained. Moreover, no degradation in landing gear emergency extension performance was observed through the use of the continuous optimized parameter values if compared with the nominal simulation results shown in fig. 7 to fig. 10, for a hydraulic fluid operational temperature of 37ºC (100ºF). For this condition, the extension times of nose and main landing gear are 6.7 seconds and 8.4 seconds, respectively.

5 Conclusions

The objective of the present work was to provide an example of modeling and simulation of a test rig airplane landing gear free-fall system applying MATLAB® software. In spite of the modeling assumptions considered, the formulation applied to construct the model yielded results that seemed to be satisfactorily representative of an airplane landing gear typical free-fall extension operation. Nowadays, the hydraulics formulation presented herein can be found implemented in several pieces of simulation software that apply a Physical Network approach, hence facilitating significantly the design process frequently performed by landing gear system engineers.

Besides running nominal simulations, the effects of hydraulic fluid low temperature operation and the presence of entrapped air in landing gear system could also be evaluated through complementary model simulations. The use of a landing gear free-fall system model to predict the impacts of these particular conditions during later aircraft operation is important to assure an acceptable system performance throughout the required flight envelope or for unusual system operational characteristics.

The impact a landing gear leg downward movement may cause to aircraft structure and the safety-related issue comprising the system capability of assuring landing gear downlocking at all foreseeable operational conditions are among the main concerns landing gear engineers have during the design of this type of system.

Therefore, a discrete optimization process, representative of the situation commonly dealt with by system designers, was firstly used to determine the best values for some model parameters in order to improve both nose and main landing gear system performance. Afterwards, an example of the application of a continuous optimization procedure was also introduced to illustrate the facilities of using the optimization algorithms currently found in simulation software like MATLAB®. Although the feasibility of the optimum solutions provided by these algorithms still needs to be validated by an engineering analysis, they might represent a good sight of the global optimum solution for the design problem, as well as being applied as a starting point for a subsequent discrete optimization process.

Consequently, the benefits of applying a virtual modeling and optimization process to reduce the possibility of system redesign in advanced stages of the product development, especially in system test rig phase, could be observed in the present work. The adoption of these processes and techniques shall be interpreted not only as a costly saving attitude, but also as a way of shortening airplane development cycle.

On the other hand, in a next step of the development process, the system model will need to be improved to consider the aerodynamic effects and eventual maneuver inertial effects expected to occur in flight. For flight conditions, other extension time values requirements might be applicable.

Finally, since aeronautical system design commonly represents a trade-off between several aspects like system performance, weight, cost, maintenance and manufacturing issues, requirements from these fields may also be considered in any optimization process.

Nomenclature

A list of the variables and parameters referred to in this article is present below.

Designation	Denotation	Unit
a	Distance between landing gear center of gravity and landing gear-to-aircraft attachment	[m]
A	Tube internal sectional area	[m^2]
A_o	Restrictor orifice or valve port area	[m^2]
A_{p1}	Piston area at actuator chamber 1	[m^2]
A_{p2}	Piston area at actuator chamber 2	[m^2]
B	Damping coefficient	[N.m.s/rad]
C_d	Discharge coefficient	
C_{ep}	Actuator external leakage coefficient	[m^3/s.Pa]
C_f	Ideal compliance	[m^3/Pa]
C_{ip}	Actuator internal leakage coefficient	[m^3/s.Pa]
D	Tube inside diameter	[m]
D_o	Restrictor orifice diameter	[m]
f	Tube friction factor	
F	Viscous friction torque	[N.m]
g	Gravitational acceleration	[m/s^2]
h	Hydraulic actuator force	[N]
H	Hydraulic actuator torque	[N.m]
I	Landing gear moment of inertia	[kg.m^2]
I_f	Inertance parameter	[kg.m^4]
K	Landing gear kinetic energy	[J]
L	Tube length	[m]
m	Landing gear mass	[kg]
P	Line pressure	[Pa]
P_1	Pressure in actuator chamber 1	[Pa]
P_2	Pressure in actuator chamber 2	[Pa]
Q	Fluid flow	[m^3/s]
Q_1	Fluid flow in the actuator chamber 1	[m^3/s]
Q_2	Fluid flow in the actuator chamber 2	[m^3/s]
r	Hydraulic actuator torque arm	[m]
Re	Reynolds number	
t	Time	[s]
T	Weight torque	[N.m]
V	Fluid velocity	[m/s]
V_G/V_T	Relative amount of trapped air	
V_1	Volume of actuator chamber 1	[m^3]
V_2	Volume of actuator chamber 2	[m^3]
α	Landing gear extension angle	[rad]
$\dot{\alpha}$	Landing gear extension velocity	[rad/s]
$\ddot{\alpha}$	Landing gear extension acceleration	[rad.s^2]
β_C	Container bulk modulus	[Pa]
β_e	Effective bulk modulus	[Pa]
β_G	Gas bulk modulus	[Pa]
β_L	Fluid bulk modulus	[Pa]
δ	Laminar flow coefficient	
ΔP	Pressure variation	[Pa]
μ	Fluid dynamic viscosity	[Pa.s]
ρ	Fluid density	[kg/m^3]

References

[1] N S Currey. *Aircraft Landing Gear Design: Principles and Practices*, AIAA Education Series, Washington, 1998, p. 373. ISBN 0930403-41-X.

[2] E Kelly. Pictures: Australian General Dynamics F-111 approved for service re-entry after June wheels-up landing. *Global International*. July, 2006. < http:// www.flightglobal.com/news/articles/pictures-australian-general-dynamics-f-111-approved-for-service-re-entry-after-june-wheels-up-landing-208102/>.

[3] Liebherr. *Landing Gear Sub System: Extension / Retraction*. <http://www.liebherr.com/AE/enGB/products_ae.wfw/id-14726-0>.

[4] Federal Aviation Administration. *Flight Test Guide for Certification of Transport Category Airplanes*. AC 25-7C. Washington: U.S Department of Transportation, 2012.

[5] M Maia Neto. *Modelagem, simulação e otimização de sistemas de extensão emergencial de trem de pouso de aeronaves*. 2011, p. 241. Dissertação de Mestrado em Sistemas Aeroespaciais e Mecatrônica – Instituto Tecnológico de Aeronáutica, São José dos Campos.

[6] E O Doebelin, *System Dynamics: Modeling, Analysis, Simulation, Design*. Marcel Dekker, New York, 1998, pp. 54-75, 206-255. ISBN 0-8247-0126-7

[7] H E Merritt. *Hydraulic Control Systems*. John Wileys and Sons, Cincinnati, Ohio, 1967. ISBN 0-471-59617-5.

[8] M Maia Neto, L C S Góes and R C M Furtado. Landing gear free-fall simulation and damping optimization using Matlab. *Inverse Problems, Design and Optimization Symposium*. João Pessoa, pp. 55-62, 2010.

[9] M Maia Neto, L C S Góes and R C M Furtado. Landing gear free-fall simulation and kinetic energy optimization. *SAE Technical Paper Series*. São Paulo, 2010, p. 14. ISSN 0148-7191.

[10] Mathworks. *SimHydraulics*: User's Guide. Natick: The MathWorks Inc, v. 1.8, 2010. <http://www. mathworks. com/help/pdf_doc/physmod/hydro/hydro_ug.pdf >.

[11] Mathworks. *Matlab*: The Language of Technical Computing (Matlab Help). Natick: The MathWorks Inc, 2007.

[12] P Venkataraman. *Applied Optimization with MATLAB® Programming*. New York: John Wiley & Sons, 2002. p. 398. ISBN 0-471-34958-5.